

# Reversible Redox Reaction Between Antiaromatic and Aromatic States of $32\pi$ -Expanded Isophlorins\*\*

Tullimilli Y. Gopalakrishna and Venkataramanarao G. Anand\*

**Abstract:**  $32\pi$ -antiaromatic expanded isophlorins with a varying number of thiophene and furan rings adopt either planar, ring-inverted, or twisted conformations depending on the number of furan rings in the macrocycle. However, they exhibit identical reactivity with respect to their oxidation to aromatic  $30\pi$ -dicationic species under acidic conditions. These  $32\pi$ -antiaromatic macrocycles can also be oxidized with  $[\text{Et}_3\text{O}^+\text{SbCl}_6^-]$  and  $\text{NOBF}_4$  to generate dications, thus confirming ring oxidation of macrocycles. Furthermore, they can be reduced back to their parent  $32\pi$ -antiaromatic state by triethylamine, Zn, or  $\text{FeCl}_2$ . Single-crystal X-ray diffraction analysis confirmed a figure-eight conformation for a hexafuran system, which opens to a planar structure upon oxidation.

Aromatic and antiaromatic forms<sup>[1]</sup> in planar conjugated systems are governed by Hückel's  $(4n + 2)$ - and  $4n\pi$ -electron rule. This empirical formula suggests the possibility of a redox-assisted interconversion between the two forms involving two  $\pi$  electrons. Such electron-transfer mechanisms coupled to proton transfer have been recently explored with expanded porphyrinoids.<sup>[2]</sup> Sessler and co-workers have shown that the  $24\pi$ -planar rosarin can be reduced to an aromatic  $26\pi$  system which in turn can be oxidized back to the parent antiaromatic macrocycle.<sup>[3]</sup> Osuka and co-workers have described the interconversion of hexaphyrins between aromatic ( $26\pi$ ) and antiaromatic ( $28\pi$ ) states by employing suitable redox agents.<sup>[4]</sup> In such porphyrinoids, the ability of the pyrrolic nitrogen atom to oscillate between the imine and amine forms is crucial to regulating the conjugated pathway for facilitating such an alteration.<sup>[3,5]</sup> In the absence of a redox process, the flexible nature of expanded porphyrinoids encourages topology-based (Hückel and Möbius) alteration between aromatic and antiaromatic states with the same number of protons and  $\pi$  electrons.<sup>[2c,6]</sup> In contrast, the  $18\pi$ -aromatic porphyrin seldom adopts the  $20\pi$ -antiaromatic form.<sup>[7]</sup> Similarly, core-modified porphyrinoids derived from tetrafulan/thiophene/selenophene/N-methylpyrrole are found to be more stable as the  $18\pi$ -aromatic dication<sup>[8]</sup> than as a neutral  $20\pi$ -antiaromatic isophlorin derivative.<sup>[9]</sup>

whereas,  $\pi$ -extended macrocycles of tetrafulan/N-methylpyrrole form stable aromatic dications.<sup>[2a,10]</sup> They may entail ring oxidation of a precursor antiaromatic macrocycle under acidic conditions in the presence of an oxidizing agent. But the reduction of the nonpyrrolic  $\pi$ -extended porphyrinoid dicationic species to the respective parent antiaromatic macrocycle has been unidentified to date. Herein we report reversible two-electron redox chemistry with isolable neutral antiaromatic and dicationic aromatic states in  $32\pi$ -expanded isophlorins.

We synthesized derivatives of the antiaromatic  $32\pi$ -expanded isophlorin<sup>[11]</sup> **1** to study their structural conformation with a varying ratio of furan and thiophene rings (Figure 1). The macrocycles **2–5** were synthesized by an

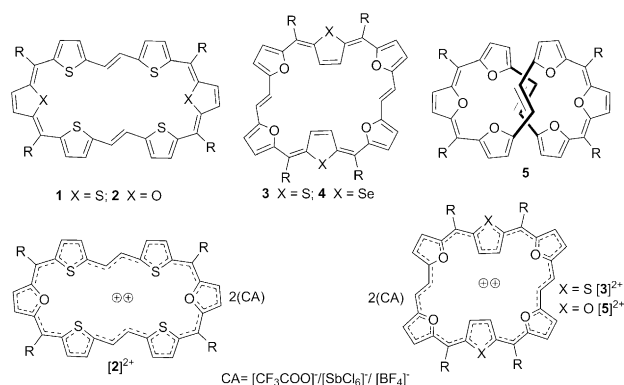


**Figure 1.** Diverse conformational features of  $32\pi$ -expanded isophlorins and their dications with a varying ratio of furan and thiophene heterocyclic units. R = pentafluorophenyl groups.

acid-catalyzed condensation of *E*-ethylene bridged bis(thiophene)/furan with the corresponding diols, followed by oxidation.<sup>[11]</sup> Apart from the expected product, very low yields of larger macrocycles were also detected in the MALDI-TOF mass spectrum of the reaction mixture. The molecules of interest could be easily purified by column chromatography. In spite of their antiaromatic nature, **2–5** do not show any sign of instability upon exposure to atmospheric conditions and can be stored for long periods of time without notable disintegration.

The composition of these macrocycles was confirmed from mass spectrometry (see the Supporting Information) and further characterized by NMR and electronic spectroscopy, as well as single-crystal X-ray diffraction studies.  $^1\text{H}$  NMR characterization of these  $32\pi$  macrocycles clearly indicated the paratropic ring current effects as expected for  $4n\pi$  systems. The compound **2** displayed four different signals

[\*] T. Y. Gopalakrishna, Prof. Dr. V. G. Anand  
Department of Chemistry  
Indian Institute of Science Education and Research (IISER)  
Pune—411008, Maharashtra (India)  
E-mail: vg.anand@iiserpune.ac.in

[\*\*] We are grateful to IISER Pune and CSIR, New Delhi, India for the financial support. T.Y.G. thanks CSIR, New Delhi, India, for a senior research fellowship.

Supporting information for this article is available on the WWW under <http://dx.doi.org/10.1002/anie.201403372>.

corresponding to an equal number of protons in the region between  $\delta = 8\text{--}5$  ppm. The protons of the thiophene rings, connected by ethylene carbon atoms, resonate as two doublets at  $\delta = 6.75$  and  $6.40$  ppm, thus suggesting weak paratropic ring current effects for the  $32\pi$  macrocycle (see the Supporting Information). A singlet for the protons of the furan ring and the ethylene bridge were observed at  $\delta = 6.31$  and  $8.01$  ppm, respectively. Unlike for **1**, the signal at  $\delta = 8.01$  ppm did not split into two signals, even at  $183$  K, thus suggesting rapid flipping of the ethylene bridge even at low temperatures. The  $^1\text{H}$  NMR spectrum of **3** at  $293$  K displayed signals in the region between  $\delta = 13\text{--}5$  ppm. A sharp singlet at  $\delta = 12.61$  ppm, a doublet at  $\delta = 4.92$  ppm, and broad signals at  $\delta = 11.80$  and  $5.43$  ppm were all indicative of the solution-state dynamics at room temperature. Upon reducing the temperature to  $220$  K, eight doublets corresponding to two protons each were observed at  $\delta = 13.24$ ,  $13.14$ ,  $12.42$ ,  $5.52$ ,  $5.28$ ,  $5.00$ ,  $4.91$ , and  $4.89$  ppm (Figure 2a). The increase in the

a variety of deuterated solvents prevented variable-temperature NMR measurements. Addition of TFA to a solution of **5** not only improved its solubility but also induced a dramatic change from the brownish-red color to a deep-blue colored solution. The mass spectrum of acidified **5** did not differ from its neutral form, thus suggesting no addition of protons to the free base (see the Supporting Information). No additional signals for the protons from the acid were observed in the well-resolved  $^1\text{H}$  NMR spectrum of **5** recorded with TFA at room temperature. It displayed three signals in the upfield region at  $\delta = -9.93$ ,  $-6.42$ , and  $-6.02$  ppm along with five other resonances in the down field region at  $\delta = 11.31$ ,  $11.42$ ,  $11.54$ ,  $12.40$ , and  $14.04$  ppm (see the Supporting Information). Since the number of signals was equal to that as observed for **3** at low temperature, a similar structural conformation can be envisaged for **5** upon addition of TFA. A large  $\Delta\delta$  value of  $24$  ppm between the proton signals of the adjacent carbon atoms clearly suggested an *E* conformation of the ethylene bridge with apparent ring current effects. Since TFA is known to act as an oxidizing agent of  $\pi$ -conjugated systems,<sup>[12]</sup> we presumed the blue colored solution to be its dication, [**5**]<sup>2+</sup>, generated by the ring oxidation of the  $32\pi$ -antiaromatic to the  $30\pi$ -aromatic macrocycle. This reaction was feasible even under inert atmosphere, thus suggesting the possibility of hydrogen evolution to complement ring oxidation through a radical mechanism. [**Et**<sub>3</sub>O<sup>+</sup>SbCl<sub>6</sub><sup>−</sup>] is well known to oxidize aromatic hydrocarbons to their respective cation radicals.<sup>[13]</sup> Recent reports have revealed the oxidation of macrocyclic oligothiophenes to respective radical cation and bipolaron

species.<sup>[14]</sup> Therefore we attempted to oxidize the ring in the absence of a proton source. It was observed that the addition of either TFA or [**Et**<sub>3</sub>O<sup>+</sup>SbCl<sub>6</sub><sup>−</sup>] to **5** displayed a similar color change and  $^1\text{H}$  NMR spectrum at room temperature. The observation of a well-resolved NMR spectrum clearly suggested the formation of diamagnetic species upon the oxidation of **5** by [**Et**<sub>3</sub>O<sup>+</sup>SbCl<sub>6</sub><sup>−</sup>] to [**5**]<sup>2+</sup>. In contrast to the oxidation of a closed-shell structure of aromatic species to radical cations, oxidizing the open-shell antiaromatic species may favor a bipolaron over radical character.

Encouraged by this observation, we recorded the  $^1\text{H}$  NMR spectra for **2** and **3** in the presence of TFA. They also displayed a remarkable change in color and NMR spectra, thus confirming an analogous modified electronic structure of the macrocycles. The  $^1\text{H}$  NMR spectrum of [**2**]<sup>2+</sup>, recorded with TFA at  $298$  K, shows two signals at  $\delta = 15.46$  and  $-9.58$  ppm for the outer and inner ethylene protons, respectively, and five other signals at  $\delta = 12.96$ ,  $11.80$ ,  $11.12$ ,  $11.02$ , and  $10.43$  ppm which correspond to the  $\beta$ -hydrogen atoms of the furans and thiophenes (see the Supporting

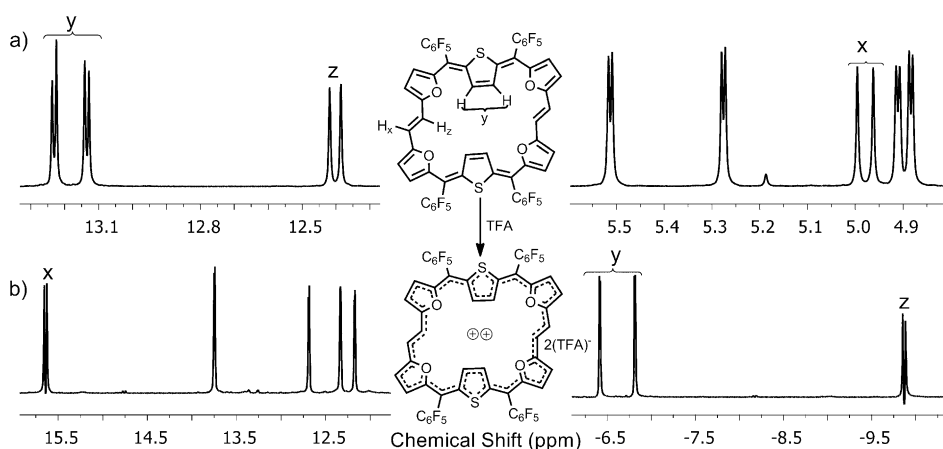


**Figure 2.** A partial view of the  $^1\text{H}$  NMR spectra of a) **3** at  $220$  K and b) [**3**]<sup>2+</sup> at  $298$  K. Peaks with a large change in their chemical shift values upon the addition of trifluoroacetic acid (TFA) to **3** are marked with the same letters. TFA<sup>−</sup> = trifluoroacetate.

number of signals signified reduced symmetry and a modified conformation of the macrocycle when the ethylene bridged thiophene subunits are replaced by furans in **1**.  $^1\text{H}$ - $^1\text{H}$  COSY spectrum revealed four sets of correlations. The calculated coupling constant for the cross-correlated signals at  $\delta = 12.42$  and  $5.00$  ppm was found to be  $16$  Hz. Combined with a  $\Delta\delta$  value of  $7.42$  ppm, it unambiguously substantiated the *E* conformation of the ethylene bridge and paratropic ring current effects expected of planar  $4n\pi$  systems. The lowfield signals at  $\delta = 13.23$  and  $13.13$  ppm, which are coupled to each other, imply an effect of paratropic ring current on the protons of the heterocyclic rings with an inverted configuration. A similar NMR signal pattern was observed for **4**, but **5** displayed a spectrum uncharacteristic of ring current effects. The  $^1\text{H}$  NMR spectrum of **5** at room temperature, revealed two doublets and two singlets in the region between  $\delta = 7.5$  and  $3.5$  ppm (see the Supporting Information). Precisely this observation suggested a highly symmetrical structure for the hexafuran macrocycle **5**, which is devoid of significant paratropic ring current effects. Poor solubility of the molecule in

Information). A  $\Delta\delta$  value of 25.0 ppm is observed between the chemical shifts of inner and outer ethylene protons. Unlike for  $[5]^{2+}$ , no doublets were observed in the upfield region thus suggesting a planar structure with no inverted rings in the dication  $[2]^{2+}$ . The  $^1\text{H}$  NMR spectrum of  $[3]^{2+}$  recorded in  $[D]TFA$  at 298 K revealed a spectral pattern akin to  $[5]^{2+}$ . Eight doublets were observed, five of which were in the lowfield region at  $\delta = 15.66$ , 13.75, 12.69, 12.34, and 12.18 ppm, and three of which were doublets in the upfield region at  $\delta = -6.41$ ,  $-6.81$ , and  $-9.85$  ppm (Figure 2b). From the  $^1\text{H}$ - $^1\text{H}$  COSY spectra it could be recognized that the proton resonances of the ring-inverted heterocycles were drastically upfield shifted to  $\delta = -6.41$  and  $-6.81$  ppm (see the Supporting Information). The two doublets at  $\delta = -9.85$  and 15.66 ppm with a coupling constant of 16 Hz correspond to the inner and outer protons of the ethylene bridge. A  $\Delta\delta$  of 25.5 ppm is found to be more than three times the difference observed ( $\Delta\delta = 7.4$  ppm) for **3**. The apparent shielding of the ring inverted protons and deshielding of the outer protons from the non-inverted rings is ascribed to the oxidation induced diatropic ring currents upon the addition of TFA.

The structure of all the macrocycles was unambiguously determined from single-crystal X-ray diffraction analysis.<sup>[15]</sup> Both **2** and  $[2]^{2+}$  show a similar arrangement of heterocycles with all the heteroatoms facing the center of the macrocycle. They crystallize in a triclinic system with a centrosymmetric P-1 space group and adopt a rectangular shape similar to that of **1**. But **2** (Figure 3a) and  $[2]^{2+}$  (see the Supporting

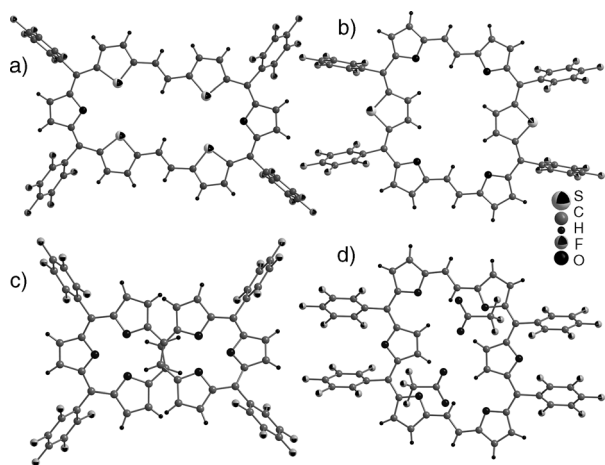


**Figure 3.** Molecular structures of a) **2**, b) **3**, c) **5**, and d)  $[5]^{2+}$  determined from single-crystal X-ray diffraction analysis. Solvent molecules are deleted for clarity.

Information) are more elongated than **1** because of the increased length between the diagonally opposite furans and a contraction between the opposite bis(thiophene) units. It was observed that the distance between the sulfur atoms of the ethylene bridged thiophenes increased from 5.62 Å in **1** to 5.96 Å in **2**. The consequent stretching of the ethylene bridge encourages its fluxional character and hence the NMR resonance of the ethylene protons could not be resolved even at 183 K. The molecular structures of **3** (Figure 3b) and **4**

(see the Supporting Information), as determined from single-crystal x-ray diffraction, exhibit a similar planar configuration and confirms their ring-inverted structures. The oxygen atoms of all the four furans point towards the center and two thiophene rings are inverted such that their  $\beta$ -carbon atoms are exposed to the center of the macrocycle. Both ethylene bridges are found to sustain an *E* conformation similar to that of the precursor bis(furan). It was observed that the large  $\pi$  surface of the bis(furan) groups are involved in offset-type  $\pi$  stacking with an interplanar distance of 3.48 Å and 3.42 Å for **3** and **4**, respectively (see the Supporting Information). Single-crystal X-ray diffraction analysis of  $[3]^{2+}$  confirmed a similar configuration as **3**, except that the  $\beta$ -carbon atoms of the thiophenes are slightly deviated from the mean macrocyclic plane (see the Supporting Information). It was also found to be associated with two trifluoroacetate ions situated at a distance of 0.89 Å above and below the ring framework, thus confirming the formation of a  $30\pi$ -aromatic dication. In stark contrast to these planar structures, **5** adopts a twisted conformation. The single-crystal X-ray diffraction analysis of **5** revealed a figure-eight configuration, with overlapping ethylene bridges and oxygen atoms of all the furans pointing towards the core of the macrocycle (Figure 3c). Even though such macrocyclic structures are observed in expanded porphyrins,<sup>[2]</sup> it represents a two-sided twisted Hückel conformation in a  $4n\pi$  isophlorinoid, thus leading to structure-induced loss of paratropicity. Hence it can be distinguished as being non-antiaromatic in nature. In a rare phenomenon, **5** transforms into a planar configuration upon the addition of TFA (Figure 3d).<sup>[5]</sup> The orientation of the heterocycles in the molecular structure of  $[5]^{2+}$  was very similar to that observed in  $[2]^{2+}$ . Two furan rings are found to be inverted such that their  $\beta$ -carbon atoms are exposed to the central cavity, while the four furans linked to the ethylene bridge orient their oxygen atoms towards the center of the macrocycle. This structural information demonstrates the dissimilar ring current effects observed in their respective  $^1\text{H}$  NMR spectra.

The nucleus independent chemical shift (NICS)<sup>[16]</sup> value was estimated for both free base and dications (see the Supporting Information). A NICS(0) value of +10.02 ppm for **2** and  $-15.31$  ppm for  $[2]^{2+}$  at their respective macrocyclic center substantiates the transformation of ring current and ring oxidation (by two electrons) into an aromatic dicationic species after the addition of TFA. A comparison of the anisotropy of the induced current density (AICD)<sup>[17]</sup> plots of **2** and  $[2]^{2+}$  revealed anticlockwise and clockwise ring current, respectively (see the Supporting Information). The plots depict an altered conjugated pathway, such that the oxygen atom of the furan rings in  $[2]^{2+}$  and sulfur atom of the thiophenes in **2** are involved along a delocalized pathway. The computed NICS(0) value for **3** and  $[3]^{2+}$  was found to be +11.24 ppm and  $-14.01$  ppm, respectively. Similar evaluation of NICS(0) for **5** gave a very low value of +1.5 ppm, thus highlighting the weak delocalization of  $\pi$  electrons in a twisted structure and hence non-antiaromatic in nature. An obscured AICD could not confirm specific ring current effects as expected in the absence of delocalization of the  $\pi$  electrons. In contrast to **5**, the estimated NICS(0) value of  $-13.9$  ppm for its dication  $[5]^{2+}$  validates the aromatic behavior in

support of experimentally verified structural features. Furthermore, its AICD plot indicated a flow of ring current in a clockwise direction, similar to that observed for  $[2]^{2+}$ .

UV/visible absorption spectra further supported the change in the electronic states of these macrocycles upon addition of TFA. The reddish-brown colored solution of **2** in dichloromethane exhibit two strong absorptions at  $\lambda = 430$  and  $482$  nm. Addition of TFA changed its color to deep-blue and absorbs at  $\lambda = 580$  and  $611$  nm with two other weak transitions in the region between  $\lambda = 800$ – $1000$  nm. A bathochromic shift by more than  $\lambda = 100$  nm and with a threefold increase in the absorption coefficient of its intense absorption band indicates a phenomenal change in the electronic character of the macrocycle. The compound **3** (Figure 4)

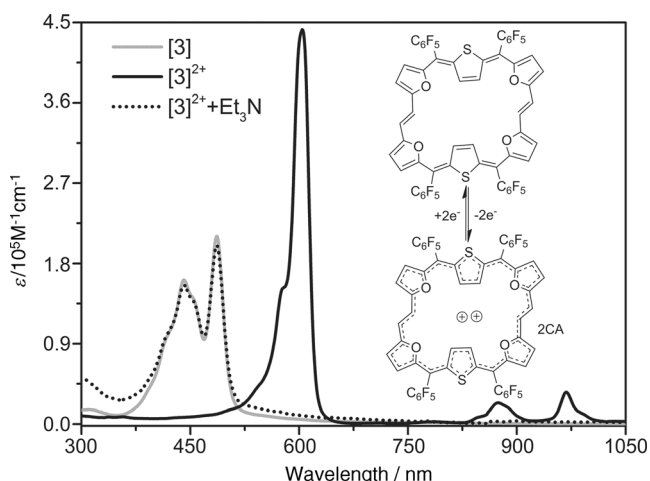


**Figure 4.** Changes in the UV/Vis absorption spectra of **3** upon the addition of TFA followed by triethylamine. CA =  $[\text{CF}_3\text{COO}]^-$ .

and **4** also show similar strong red-shifted absorption upon the addition of TFA. Controlled addition of TFA to a solution of **3** in dichloromethane indicated a one-to-one conversion of the macrocycle into its corresponding dication (see the Supporting Information). The addition of oxidizing agents such as  $[\text{Et}_3\text{O}^+\text{SbCl}_6^-]$  and  $\text{NOBF}_4$  to **3** in dichloromethane also display similar  $^1\text{H}$  NMR and absorption spectra (see the Supporting Information). But, addition of DDQ alone did not induce any change in the absorption spectrum. **5** also shows two close intense absorptions at  $\lambda = 467$  and  $499$  nm along with a high-energy shoulder at around  $\lambda = 450$  nm. Such strong absorptions may be attributed to the possible Möbius aromaticity of the twisted macrocycle.<sup>[18]</sup> The generated  $[\mathbf{5}]^{2+}$  undergoes a  $150$  nm red-shift to show an intense absorption at  $\lambda = 610$  nm followed by weak transitions in the region between  $\lambda = 800$ – $1000$  nm (see the Supporting Information). Quantum chemical calculations revealed relative stabilization of the HOMO and LUMO in the dications compared to their corresponding neutral macrocycles (see the Supporting Information). The relatively broad bands for the neutral macrocycles, compared to the sharp absorptions of aromatic dications, further justifies the change in the  $\pi$ -electron count from  $4n$  to  $(4n+2)$ .<sup>[19]</sup> This finding further substantiates

a stable aromatic state relative to its analogous antiaromatic state. The dications of **2**, **3**, **4**, and **5** are stable under ambient conditions and quite inert to moisture. But, addition of triethylamine to  $[\mathbf{5}]^{2+}$  changed the deep-blue solution to the original reddish-brown color with the same absorption features as of **5** (see the Supporting Information), thus confirming the twisting of a planar molecule into a figure-eight conformation. The compounds **2**, **3**, and **4** also show similar interconversion, thus exemplifying acid-base induced conformational exchange in an antiaromatic expanded isophlorinoid (see the Supporting Information). Triethylamine acts as an electron donor<sup>[20]</sup> to reduce the cationic species through the formation of its own radical cation and hence completes the cycle of interconversion between antiaromatic and aromatic states through a redox process. Apart from triethylamine,  $\text{FeCl}_2$  and zinc also reduce dicationic species to the neutral antiaromatic systems. The earlier reported tetraoxaporphyrin dications/dianions transform into the neutral and air-sensitive  $20\pi$  isophlorins only with strong reducing or oxidizing agents under inert atmosphere.<sup>[8a]</sup> Our own earlier reports show that  $20\pi$  isophlorins can be oxidized to unstable  $18\pi$  systems only under harsh reaction conditions.<sup>[21]</sup> Preliminary cyclic voltammetric studies of **3** shows a reversible oxidation signal and reduction signal at  $+0.5$  V and  $-1.0$  V, respectively (see the Supporting Information). The compound **2** also displays similar signals in its cyclic voltammogram. It is possible that the two oxidation potentials are within a  $100$  mV difference and hence could not be resolved into individual signals.

In summary,  $32\pi$ -antiaromatic expanded isophlorins show remarkable structural diversity and are susceptible to ring oxidation to form stable aromatic dications. For the first time, we have shown redox-dependent interchangeable conformations for an expanded isophlorin. Spectroscopic analysis, single-crystal X-ray diffraction studies, and quantum chemical calculations reveal the formation of stable aromatic dications upon the addition of TFA,  $[\text{Et}_3\text{O}^+\text{SbCl}_6^-]$ , or  $\text{NOBF}_4$ . In contrast to the generation of radicals from aromatic systems,  $[\text{Et}_3\text{O}^+\text{SbCl}_6^-]$  or  $\text{NOBF}_4$  tend to oxidize antiaromatic systems to aromatic dicationic species. These dications can be reduced to their neutral antiaromatic state by a variety of reducing agents such as zinc,  $\text{FeCl}_2$ , or triethylamine. In spite of the apparent thermodynamic stability for aromaticity, the reversible process between  $4n\pi$  and  $(4n+2)\pi$  states may be attributed to the facile reduction of aromatic dicationic species towards a neutral antiaromatic state. This study represents a prime example of an antiaromatic isophlorinoid and its corresponding aromatic dication as a reversible couple to interconvert amongst themselves with suitable redox reagents.

Received: March 16, 2014

Revised: April 21, 2014

Published online: May 14, 2014

**Keywords:** aromaticity · electron transfer · heterocycles · macrocycles · porphyrinoids



- [1] a) R. Breslow, *Chem. Eng. News* **1965**, 43, 90; b) R. Breslow, *Acc. Chem. Res.* **1973**, 6, 393; c) A. D. Allen, T. T. Tidwell, *Chem. Rev.* **2001**, 101, 1333; d) F. Sondheim, *Acc. Chem. Res.* **1972**, 5, 81; e) P. J. Garratt, *Aromaticity*, Wiley, New York, **1986**.
- [2] a) J. L. Sessler, D. Seidel, *Angew. Chem.* **2003**, 115, 5292; *Angew. Chem. Int. Ed.* **2003**, 42, 5134; b) S. Saito, A. Osuka, *Angew. Chem.* **2011**, 123, 4432; *Angew. Chem. Int. Ed.* **2011**, 50, 4342; c) M. Stepien, N. Sprutta, L. Latos-Grazynski, *Angew. Chem.* **2011**, 123, 4376; *Angew. Chem. Int. Ed.* **2011**, 50, 4288; d) T. K. Chandrashekar, S. Venkatraman, *Acc. Chem. Res.* **2003**, 36, 676.
- [3] M. Ishida, S. J. Kim, C. Preihs, K. Ohkubo, J. M. Lim, B. S. Lee, J. S. Park, V. M. Lynch, V. V. Roznyatovskiy, T. Sarma, P. K. Panda, C. H. Lee, S. Fukuzumi, D. Kim, J. L. Sessler, *Nat. Chem.* **2013**, 5, 15.
- [4] a) T. Tanaka, N. Aratani, A. Osuka, *Chem-Asian J.* **2012**, 7, 889; b) M. Inoue, A. Osuka, *Angew. Chem.* **2010**, 122, 9678; *Angew. Chem. Int. Ed.* **2010**, 49, 9488.
- [5] G. Karthik, J. M. Lim, A. Srinivasan, C. H. Suresh, D. Kim, T. K. Chandrashekar, *Chem. Eur. J.* **2013**, 19, 17011.
- [6] a) J. Sankar, S. Mori, S. Saito, H. Rath, M. Suzuki, Y. Inokuma, H. Shinokubo, K. Suk Kim, Z. S. Yoon, J.-Y. Shin, J. M. Lim, Y. Matsuzaki, O. Matsushita, A. Muranaka, N. Kobayashi, D. Kim, A. Osuka, *J. Am. Chem. Soc.* **2008**, 130, 13568; b) S. Saito, J.-Y. Shin, J. M. Lim, K. S. Kim, D. Kim, A. Osuka, *Angew. Chem.* **2008**, 120, 9803; *Angew. Chem. Int. Ed.* **2008**, 47, 9657; c) M. Stępień, B. Szyszko, L. Latos-Grażyński, *J. Am. Chem. Soc.* **2010**, 132, 3140.
- [7] R. B. Woodward, *Angew. Chem.* **1960**, 72, 651.
- [8] a) E. Vogel, *Pure Appl. Chem.* **1993**, 65, 143; b) M. Pohl, H. Schmickler, J. Lex, E. Vogel, *Angew. Chem.* **1991**, 103, 1737; *Angew. Chem. Int. Ed. Engl.* **1991**, 30, 1693; c) E. Vogel, W. Haas, B. Knipp, J. Lex, H. Schmickler, *Angew. Chem.* **1988**, 100, 445; *Angew. Chem. Int. Ed. Engl.* **1988**, 27, 409; d) E. Vogel, C. Fröde, A. Breihan, H. Schmickler, J. Lex, *Angew. Chem.* **1997**, 109, 2722; *Angew. Chem. Int. Ed.* **1997**, 36, 2609; e) E. Vogel, P. Rohrig, M. Sicken, B. Knipp, A. Herrmann, M. Pohl, H. Schmickler, J. Lex, *Angew. Chem.* **1989**, 101, 1683; *Angew. Chem. Int. Ed. Engl.* **1989**, 28, 1651.
- [9] a) J. A. Cissell, T. P. Vaid, A. L. Rheingold, *J. Am. Chem. Soc.* **2005**, 127, 12212; b) C. Liu, D.-M. Shen, Q.-Y. Chen, *J. Am. Chem. Soc.* **2007**, 129, 5814; c) A. Weiss, M. C. Hodgson, P. D. W. Boyd, W. Siebert, P. J. Brothers, *Chem. Eur. J.* **2007**, 13, 5982.
- [10] a) B. Franck, A. Nonn, *Angew. Chem.* **1995**, 107, 1941; *Angew. Chem. Int. Ed. Engl.* **1995**, 34, 1795; b) V. Markl, T. Knott, P. Kreitmeier, T. Burgemeister, F. Kastner, *Helv. Chim. Acta* **1998**, 81, 1480; c) G. Markl, R. Ehrl, H. Sauer, P. Kreitmeier, T. Burgemeister, *Helv. Chim. Acta* **1999**, 82, 59.
- [11] T. Y. Gopalakrishna, J. S. Reddy, V. G. Anand, *Angew. Chem.* **2013**, 125, 1807; *Angew. Chem. Int. Ed.* **2013**, 52, 1763.
- [12] a) J. A. E. H. Van Haare, L. Groenendaal, E. E. Havinga, R. A. J. Janssen, E. W. Meijer, *Angew. Chem.* **1996**, 108, 696; *Angew. Chem. Int. Ed. Engl.* **1996**, 35, 638; b) A. J. Bard, A. Ledwith, H. J. Shine, *Adv. Phys. Org. Chem.* **1976**, 13, 155; c) J. J. Dannenberg, *Angew. Chem.* **1975**, 87, 632; *Angew. Chem. Int. Ed. Engl.* **1975**, 14, 641.
- [13] R. Rathore, A. S. Kumar, S. V. Lindeman, J. K. Kochi, *J. Org. Chem.* **1998**, 63, 5847.
- [14] a) F. Zhang, G. Gotz, E. Mena-Osteritz, M. Weil, B. Sarkar, W. Kaim, P. Bauerle, *Chem. Sci.* **2011**, 2, 781; b) M. Iyoda, K. Tanaka, H. Shimizu, M. Hasegawa, T. Nishinaga, T. Nishiuchi, Y. Kunugi, T. Ishida, H. Otani, H. Sato, K. Inukai, K. Tahara, Y. Tobe, *J. Am. Chem. Soc.* **2014**, 136, 2389.
- [15] CCDC 983662 (2), 983663 ([2]<sup>2+</sup>), 983664 (3), 983665 ([3]<sup>2+</sup>), 983666 (4), 983667 (5), and 983668 ([5]<sup>2+</sup>) contain the supplementary crystallographic data for this paper. These data can be obtained free of charge from The Cambridge Crystallographic Data Centre via [www.ccdc.cam.ac.uk/data\\_request/cif](http://www.ccdc.cam.ac.uk/data_request/cif).
- [16] P. von R. Schleyer, C. Maerker, A. Dransfeld, H. J. Jiao, N. J. R. van Eikema Hommes, *J. Am. Chem. Soc.* **1996**, 118, 6317.
- [17] D. Geuenich, K. Hess, F. Kohler, R. Herges, *Chem. Rev.* **2005**, 105, 3758.
- [18] T. Higashino, A. Osuka, *Chem. Sci.* **2013**, 4, 1087.
- [19] S. Cho, Z. S. Yoon, K. S. Kim, M. C. Yoon, D. G. Cho, J. L. Sessler, D. Kim, *J. Phys. Chem. Lett.* **2010**, 1, 895.
- [20] a) N. L. Weinberg, H. R. Weinberg, *Chem. Rev.* **1968**, 68, 449; b) L. C. Porits, V. V. Bhat, C. K. Mann, *J. Org. Chem.* **1970**, 35, 2175; c) Y. L. Chow, W. C. Danen, S. F. Nelsen, D. H. Rosenblatt, *Chem. Rev.* **1978**, 78, 243.
- [21] J. S. Reddy, V. G. Anand, *J. Am. Chem. Soc.* **2008**, 130, 3718.